



Divergent carbon use efficiency-growth rate tradeoff in popular biological growth models

Jinyun Tang, William J. Riley, Gianna L. Marschmann and Eoin L. Brodie

5 Department of Molecular Ecology and Biogeochemistry, Climate and Ecosystem Science Division, Lawrence Berkeley National Laboratory, Berkeley, CA, USA.

Correspondence to: Jinyun Tang jinyuntang@lbl.gov

Running title: Divergent CUE.

10

Abstract. Carbon use efficiency (CUE) is an important trait emerging from processes regulating biological growth. CUE can be computed either based on the growth of structural biomass or total biomass divided by substrate uptake rate. Nonequilibrium thermodynamics and observations suggest that, for an exponentially growing population, structural biomass CUE should first increase, then peak, and finally decrease with specific growth rate; meanwhile, total biomass CUE increases asymptotically with specific growth rate. We compared predictions from six popular models that are often used for plant and microbial growth in existing ecosystem models. We found that, for an exponentially growing population of biological cells, (1) the Pirt model and Compromise model predict that structural biomass CUE increase asymptotically with growth rate; (2) the modified Droop model predicts that structural biomass CUE decreases with growth rate; and (3) the variable internal storage model and two dynamic energy budget models predict that structural biomass CUE first increases, then peaks, and finally decreases with growth rate. Moreover, the modified Droop model predicts that total biomass CUE is constant with growth rate, while all other five models predict that total biomass CUE increases with growth rate asymptotically. For non-exponential biological growth, we show that there is no deterministic relationship between total biomass CUE or structural biomass CUE with respect to either growth rate or temperature. Therefore, we contend that biological growth models should explicitly represent interactions between substrate acquisition, substrate transformation, and maintenance respiration to better capture observed CUE dynamics and thereby ecosystem biogeochemistry.

1 Introduction

For a growing biological organism, carbon use efficiency (CUE) is defined as the fraction of a unit mass of newly captured carbon that is retained as newly synthesized biomass (for simplicity, our discussion here regards all excreted organic polymers, such as exoenzymes, as part of the total biomass), while the remaining uptake is respired to support this growth (e.g., Manzoni et al., 2018). Because the carbon used to support new biomass synthesis also fulfills the metabolic needs of maintaining existing structural biomass, and, due to environmental fluctuations, the cost of such maintenance is generally dynamic, CUE is inferred to be dynamic even for an organism that is of fixed chemical elemental stoichiometry. Nevertheless, biogeochemical (BGC) models differ widely in their representation of CUE, for example, as a constant parameter (Wieder et al., 2015), a deterministic function of various regulating factors (e.g., temperature, macronutrient concentration; Allison et al., 2010), or an emergent variable that changes according to the chosen way of analysis (Tang and Riley, 2015; Manzoni et al., 2018; Allison, 2025). Moreover, a few studies using variable internal storage models differentiated between structural and reserve biomass (e.g.,



Tang and Riley, 2015; Kooijman, 2009; Nev and Van Den Berg, 2017), and reasoned that, since only the structural biomass requires maintenance, CUE can be either defined with respect to the growth of structural biomass or total biomass. However, models that do not differentiate between structural biomass and reserve biomass (e.g., all microbe-implicit soil BGC models; Koven et al., 2013; Parton et al., 1988; Jenkinson, 1990), the Pirt model (Pirt, 1982), and the Compromise model (Beefink et al., 1990; Wang and Post, 2012)) implicitly assume an equal CUE for structural and total biomass growth.

In the modeling of soil organic matter decomposition dynamics, CUE defined for the representative microbe in a population is regarded as an essential parameter to determine how much carbon can be retained in soils after respiration. Recently, using a linear turnover pool-based soil carbon model, Tao et al. (2023) highlighted microbial CUE as the most important parameter to better constrained to improve the estimation of global soil carbon storage (by the microbe-implicit model they used). Meanwhile, microbe-explicit soil BGC models are demonstrating more diverse variations of predicted microbial CUE (some of their prototypes are analyzed later in this manuscript). In general, these microbe-explicit models can be organized into four classes: (1) the Herbert model (Dawes and Ribbons, 1964), (2) the Pirt-model (Pirt, 1982, 1965), (3) the Compromise model (Beefink et al., 1990), and (4) variable internal storage models, including the plant growth model by Thornley (1972), dynamic energy budget models (Tang and Riley, 2015, 2023; Kooijman, 2009), and the Droop model (Thingstad, 1987). We note that because the variable internal storage models have both structural and reserve biomass, their CUE may be computed in two different ways by either focusing on structural biomass or total biomass. Since it is the structural biomass that represents the effect of microbial population on substrate uptake, it is important to recognize how the way of CUE computation affects the interpretation of CUE dynamics.

Since plants are structurally more complex than microbes, the CUE dynamics during plant growth is also more complicated. Theoretically, the whole plant CUE should be defined as the fraction of allocated carbon to various organs that becomes newly synthesized biomass (Thornley, 1972). Because the relative carbon allocation to each plant organ varies with environmental conditions and different organs usually have different CUE, whole plant CUE is generally dynamic (Manzoni et al., 2018). Even when all plant organs are assumed to have the same CUE, the dynamics of relative carbon allocation for maintenance and growth will still result in dynamic whole plant CUE. In the literature, the mean whole plant CUE is often quantified as the ratio of net primary productivity to gross primary productivity (Sinsabaugh et al., 2017), and has been mapped for some regions using remote sensing imagery (Bloom et al., 2016; Zhang et al., 2009) and field data (Liu et al., 2022).

Conceptually, biological growth is thermodynamically controlled and therefore naturally resembles how a thermal or mechanical engine works with its supplied energy (Roach et al., 2018). For a Carnot thermal engine, classical thermodynamics has shown that its energy use efficiency has an upper bound of $1 - T_L/T_H$, with T_L and T_H being the low and high temperatures of two heat reservoirs, respectively (Feynman et al., 2011). However, this classical thermodynamic result assumes that all processes are reversible. That is, the engine is working so slowly that its power is *de facto* zero. This assumption disagrees with the empirical observation (and desire) that a working engine should be able to deliver a finite amount of work during any given time. Thus, nonequilibrium thermodynamics was developed to analyze the efficiency of various engines (Bejan, 1996; Andresen et al., 1977; Andresen et al., 1984; Onsager, 1931b, a). One important inference from nonequilibrium thermodynamics is that there exists a tradeoff between power and energy efficiency of an engine, so that one sub-optimal efficiency may correspond to both a low and high input power (Roach et al., 2018; Yuan et al., 2022).

The real-life experience of driving can help understand the power-yield tradeoff mentioned above. In this example, the yield is fuel use efficiency (FUE), i.e., distance traveled per volume fuel consumed by an internal combustion vehicle (e.g., km per liter gas). When a vehicle's engine is off, its output power is zero, and the vehicle has zero FUE. When the engine is on but the car is not moving, FUE is still zero (and the fuel use just keeps the engine idling). When the vehicle gradually accelerates on



a flat road, FUE gradually increases, and then stabilizes at a value that is more or less as advertised by the vehicle manufacturer. When the driver is overtaking another vehicle or climbing a slope, greater power is demanded. This is done by pressing the pedal (and probably shifting the gear into sport mode at the same time), so that the vehicle may pick up further speed (with the greater power) at the cost of lower FUE. However, in the real-world, because conditions where a car operates usually fluctuate widely, one is more likely to find the car's power-yield tradeoff varies continuously. We note that internal combustion engines generally cannot store the energy produced from burning the fuel, thus this energy is either wasted or used for moving the vehicle. A hybrid vehicle may store some of the kinetic energy generated from fuel burning for later use. As we will see later, biological cells work more likely a hybrid vehicle. Consistent with this analogy, for mean values based on 398 observations of foreign and US domestic automobiles from the model years 1970 to 1982, Boland and Schreyer (2024) found a clear decrease of FUE with increasing horsepower.

Although biological organisms and vehicles' mechanical engines use energy in different forms, they must adhere to the same thermodynamic principles. Therefore, it is reasonable to infer that the CUE of biological growth should also be a dynamic variable, and follow a similar power-yield tradeoff. This pattern has been hypothesized for microbial CUE by Lipson (2015) based on a synthesis of empirical studies from the literature, and was predicted by the dynamic energy budget models (Tang and Riley, 2023, 2025).

Considering the significance of CUE in predicting ecosystem biogeochemistry, it is important to answer the following questions: are the formulations commonly used by existing ecosystem biogeochemical models representing CUE dynamics consistently with thermodynamics? If not, what important features could have been missed by those formulations? In the following sections we analyze the tradeoff between growth rate and CUE in six mathematical formulations, some of which underlie most existing ecosystem biogeochemical models. We then highlight the importance of resolving the growth rate-CUE tradeoff dynamically and discuss how it can be properly formulated in future models.

2 Theory

We first introduce a modified version of the model used by Odum and Pinkerton (1955) for their analysis of diverse systems that involve the coupling between energy supply and energy use. We describe that model to illustrate the generic features of coupled energy supply and use as implied by nonequilibrium thermodynamics. Then we introduce the biological growth models that are used in many ecosystem models, and analyze the relationship between growth rate and CUE implied by those growth models. All mathematical symbols are described in Table A1.

2.1 The modified Odum-Pinkerton model

The model is formulated using Onsager's reciprocal relations (Onsager, 1931b):

$$J_1 = (l + cf^2)X_1 - cfX_2, \quad (1)$$

$$J_2 = -cfX_1 + (c + \epsilon)X_2, \quad (2)$$

$$T \frac{dS_e}{dt} = J_1X_1 + J_2X_2. \quad (3)$$

In the above model, l , f , c and ϵ are constant parameters (whose definitions depend on the application), X_1 and X_2 are forces, J_1 is the flux into the system under the influence of force X_1 , and J_2 is the flux output with force X_2 . The sum of products of fluxes and forces contributes to the heat dissipation of the system as measured by the entropy production rate dS_e/dt multiplied with temperature T in equation (3). Note that equation (3) follows directly from the first law of thermodynamics (aka



energy conservation), so that given the power input $P_1 = J_1 X_1$, and the heat dissipation rate $T \frac{dS_e}{dt}$, the useful power output is $P_2 = -J_2 X_2$. Consequently, the system's energy use efficiency (η) is

$$\eta = \frac{P_2}{P_1} = \left(1 + \frac{l}{cf^2} - p\right) \left(1 - \frac{l}{pcf^2} - \frac{\epsilon}{c} \left(\frac{l+cf^2}{pcf^2} - 1\right)\right), \quad (4)$$

where $p = P_1/c(fX_1)^2$. Further, we note that

$$p = \frac{P_1}{c(fX_1)^2} = \left(1 + \frac{l}{cf^2}\right) - \frac{X_2}{fX_1} < 1 + \frac{l}{cf^2}, \quad (5)$$

so that η may vary from being negative to a positive maximum value. Particularly, when η is plotted against p , we obtain the non-monotonic tradeoff curve (Figure 1).

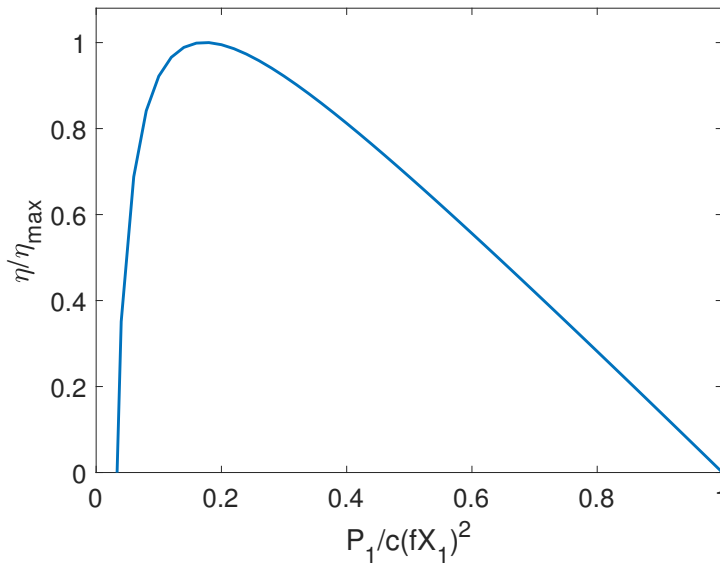


Figure 1. The power-yield tradeoff predicted by the modified Odum-Pinkerton model. Here, we set $l = 0$ and $\epsilon = 0.03$, so that the model is describing the 7th example in Odum and Pinkerton (1955), which represents an organism that captures and uses food for its maintenance and growth, except that we here assume that the maintenance cost is paid by X_2 (analogous to the reserve biomass in the variable internal storage models, e.g., the DEB models in this study).

Odum and Pinkerton (1955) (hereafter OP1955) used the above model to analyze (1) Atwood's machine (e.g., Monteiro et al., 2015), (2) a water wheel turning a grindstone, (3) one battery charging another battery, (4) a thermocouple running an electric motor, (5) a thermal diffusion engine, (6) the metabolism of a pseudo-organism (with no self-repair), (7) food capture by an organism for its maintenance and growth, (8) a model of photosynthesis, (9) primary production in a self-sustaining climax community, and (10) growth and maintenance of a civilization. Among them, the 7th example is closest to the biological growth we discuss here. (Moreover, the fact that these equations can describe so many types of systems suggests what can be inferred from these equations for the energy use efficiency is a universal feature that is guaranteed by nonequilibrium thermodynamics. Consequently, the 7th example and the subject of our analysis—biological growth—should have the same characteristics in terms of energy use.) For this example, specifically, J_1 describes the rate of food assimilation, X_1 corresponds to the energy drop in metabolism of captured food units (thus X_1 represents the energy quality of the substrate taken from the environment), J_2 represents the rate of effective food capture, X_2 is the energy drop inherent in the capture of a unit of food (thus X_2 is analogous to the reserve biomass in the DEB models), l designates the basal metabolism spent in self-repair (as paid by X_1 in the original



OP1955 formulation), and c is related to the effectiveness of food concentrating method, f is metabolic equivalent of the food capture process. However, considering that biological organisms may keep respiring in the absence of food uptake (aka when $J_1 = 0$; e.g., Dawes and Ribbons (1964)), it is more reasonable to pay the basal metabolism with X_2 , so that $l = 0$ while $\epsilon > 0$.

135 Nonetheless, this change does not alter the non-monotonic tradeoff between efficiency η and the input power P_1 (Figure 1). Moreover, in the OP1955 model, all input power P_1 goes to output power P_2 and waste, thus there is no change in storage energy density. Therefore, the implied non-monotonic power-yield tradeoff corresponds to exponential biological growth, as discussed below.

2.2 Biological growth models

140 We next analyze six biological growth models: (1) Pirt model (Pirt, 1965), (2) Compromise model (Beefink et al., 1990), (3) Modified Droop (mDroop) model (Thingstad, 1987), (4) Variable Internal Storage (VIS) model modified from Thornley's plant model (Thornley, 1972), (5) the standard dynamic energy budget (sDEB) model (Kooijman, 2009), and (6) the modified dynamic energy budget (mDEB) model (Tang and Riley, 2025). Both the Pirt and Compromise models consider a single biomass pool, and treat growth and maintenance as independent processes, having the same priority in using the substrate.
 145 As the growth in the Pirt model and Compromise model is directly driven by substrate uptake, they are in the category of source-driven growth models (Fatichi et al., 2014). The other four models assume biomass consists of structural and reserve biomass. Among them, the VIS, sDEB and mDEB models drive structural biomass growth using reserve biomass, thus they are in the category of sink-driven models (Fatichi et al., 2014). Following Thingstad (1987), the mDroop model has the most parameters, and uses the total biomass to compute the growth rate (through the total-biomass-based substrate quota, even though it does have
 150 reserve biomass), thus it is a sink-driven model only apparently. For the Pirt and Compromise models, their equations stay the same as in Table 1. The general forms of the other four models differ from those (for exponential growth) in Table 1 and are detailed (from section A to D) in the supplemental material.

We compared the six models' predictions of CUE dynamics for (1) an exponentially growing population under constant carbon inputs using equations in Table 1, (2) 50-year simulations using equations from section E of the supplemental material
 155 that mimic microbe-driven soil carbon dynamics under month-to-month varying carbon inputs (generated by random perturbations around the base annual input rate of 350 gC yr⁻¹, with a standard deviation of 50 gC yr⁻¹ and fixed monthly allocation; Figure S1a), and (3) 50-year simulations that further consider the influence of intra-day temperature variations (Figure S1b) on related temperature-dependent kinetic parameters (whose parameterizations are detailed in section F of the supplemental material).

160

165



170

Table 1. Models for exponential biological growth $\mu(S)$ as a function of substrate uptake $q(S)$. Listed in parentheses by each model's name are key model parameters, whose definitions are detailed in the nomenclature Table in Appendix A. Notably, Y_V and Y_B are CUEs for structural biomass and total biomass, respectively, both of which are normalized with substrate assimilation efficiency Y_S . More detailed model descriptions are in the supplemental material.

Pirt model: $(\mu_{max}, m_V, Y_S), h(S)$	Pirt (1965, 1982)
$\mu(S) = \mu_{max} h(S)$ $q(S) = \frac{\mu}{Y_S} + \frac{m_V}{Y_S} = \frac{\mu}{Y_S} \left(1 + \frac{m_V}{\mu} \right)$ $\frac{Y_V}{Y_S} = \frac{Y_B}{Y_S} = \frac{\mu(S)}{q(S)Y_S} = \frac{\mu}{\mu + m_V}$	
<p>Description: This model assumes that specific growth rate $\mu(S)$ is down-regulated linearly from the maximum growth rate μ_{max} by the substrate response function $h(S)$. Substrate taken up $q(S)$ is partitioned between that for biomass synthesis μ/Y_S and maintenance m_V/Y_S. As a single biomass compartment model, its structural biomass yield Y_V and total biomass yield Y_B are equal.</p>	
Compromise (Comp) model: $(\mu_{max}, m_V, Y_S), h(S)$	Wang and Post (2012)
$\mu(S) = \mu_{max} h(S) - m_V [1 - h(S)]$ $q(S) = \frac{\mu}{Y_S} + \frac{m_V}{Y_S}$ $\frac{Y_V}{Y_S} = \frac{Y_B}{Y_S} = \frac{\mu(S)}{q(S)Y_S} = \frac{\mu}{\mu + m_V}$	
<p>Description: This model assumes that specific growth rate $\mu(S)$ consists of two parts, where the first part linearly scales the maximum growth rate μ_{max} with the substrate response function $h(S)$, and the second part signifies negative growth due to maintenance $m_V[1 - h(S)]$ that decreases linearly with the substrate response function $h(S)$. Substrate taken up $q(S)$ is partitioned between that for biomass synthesis μ/Y_S and maintenance m_V/Y_S. As a single-biomass-compartment model, its structural biomass yield Y_V and total biomass yield Y_B are equal.</p>	
Modified Droop (mDroop) model: $(\mu_{max}, c_1, c_2, Q_{min}, Q_{max}, Y_S), j_A(S)$	Thingstad (1987)
$\mu(S) = \frac{\mu_{max} j_A (Q_{max} - Q_{min})}{j_A Q_{max} + [c_2 + (1 + c_1) \mu_{max}] Q_{min} (Q_{max} - Q_{min})}$ $q(S) = \frac{(1 + c_1) \mu_{max} + c_2}{\mu_{max} - \mu} \frac{Q_{min}}{Y_S} \mu$ $\frac{Y_V}{Y_S} = \frac{\mu_{max} - \mu}{(1 + c_1) \mu_{max} + c_2 Q_{min}} \frac{1}{\mu}$ $\frac{Y_B}{Y_S} = \frac{\mu_{max}}{(1 + c_1) \mu_{max} + c_2}$	
<p>Description: This model assumes that specific growth rate $\mu(S)$ is linearly down-regulated from the maximum growth rate μ_{max} by the carbon quota function $1 - Q_{min}/Q$, where the carbon quota Q is defined as the ratio between total biomass B_X and structural biomass B_V (see eq.(A3) in section A of the supplemental material). The total biomass B_X increases due to substrate uptake $j_A \frac{Q_{max}-Q}{Q_{max}-Q_{min}} B_V$, and decreases due to respiration $R B_V$ (see eq. A(2) in the supplemental material), where the specific respiration R is a linear function of specific growth rate $\mu(S)$, whose coefficients depend linearly on carbon quota (eq.(A5) in the supplemental material). As a two-biomass-compartment model, its total biomass yield Y_B and structural biomass yield Y_V differ, and they can be analytically represented as a function of specific growth rate μ only for an exponentially growing population.</p>	
Variable-internal-stores (VIS) model: $(v_E, m_V, Y_S, Y_{RV}), j_A(S)$	Williams (1967); Thornley (1972)
$\mu(S) = \frac{v_E}{2} \left(-1 + \sqrt{1 + \frac{4(j_A Y_S - m_V) Y_{RV}}{v_E}} \right)$	



$$q(S) = \frac{\mu}{Y_S Y_{RV}} \left(1 + \frac{\mu}{v_E}\right) + \frac{m_V}{Y_S}$$

$$\frac{Y_V}{Y_S} = \frac{v_E \mu}{(v_E + \mu) \mu + v_E m_V Y_{RV}} Y_{RV}$$

$$\frac{Y_B}{Y_S} = \frac{(v_E Y_{RV} + \mu) \mu}{(v_E + \mu) \mu + v_E m_V Y_{RV}} Y_S$$

Description: This model assumes that reserve biomass B_X is mobilized to parallelly meet the demand from maintenance and growth of structural biomass B_V (see eq. (B1) in section B of the supplemental material). As a two-biomass-compartment model, its total biomass yield Y_B and structural biomass yield Y_V differ, and they can be analytically represented as a function of specific growth rate μ only for an exponentially growing population.

Standard dynamic energy budget (sDEB) model: $(v_E, m_V, Y_S, Y_{RV}), j_A(S)$ Tang and Riley (2023); Kooijman (2009)

$$\mu(S) = \frac{Y_{RV} Y_S j_A - m_V}{1 + Y_{RV} Y_S j_A / v_E}$$

$$q(S) = \frac{v_E (m_V + \mu)}{Y_S Y_{RV} (v_E - \mu)}$$

$$\frac{Y_V}{Y_S} = \frac{\mu}{\mu + m_V} \left(1 - \frac{\mu}{v_E}\right) Y_{RV}$$

$$\frac{Y_B}{Y_S} = \left(\frac{\mu}{\mu + m_V}\right) \left(\frac{Y_{RV} v_E + m_V + (1 - Y_{RV}) \mu}{v_E}\right)$$

Description: This model assumes that, when the reserve biomass B_X is mobilized to meet the demand from maintenance first and then the growth of structural biomass B_V , the reserve density (i.e. B_X/B_V) follows the first order kinetics (eq. (C1) in section C of the supplemental material). As a two-biomass-compartment model, its total biomass yield Y_B and structural biomass yield Y_V differ, and they can be analytically represented as a function of specific growth rate μ only for an exponentially growing population.

Modified dynamic energy budget (mDEB) model: $(v_E, m_V, Y_S, Y_{RV}), j_A(S)$ Tang and Riley (2025)

$$\mu(S) = \frac{m_V + v_E}{2} \left(-1 + \sqrt{1 + \frac{4 v_E (j_A Y_S Y_{RV} - m_V)}{(m_V + v_E)^2}}\right)$$

$$q(S) = \left(1 + \frac{\mu}{v_E}\right) \left(\frac{\mu + m_V}{Y_{RV} Y_S}\right)$$

$$\frac{Y_V}{Y_S} = \left(\frac{\mu}{\mu + m_V}\right) \left(\frac{v_E}{v_E + \mu}\right) Y_{RV}$$

$$\frac{Y_B}{Y_S} = \left(\frac{\mu}{\mu + m_V}\right) \left(\frac{Y_{RV} v_E + \mu + m_V}{v_E + \mu}\right)$$

Description: This model assumes that reserve biomass B_X is mobilized kinetically to meet the demand from maintenance first and then the growth of structural biomass B_V . Unlike the sDEB model, it does not restrict the reserve density (i.e. B_X/B_V) to follow the first order kinetics. As a two-biomass-compartment model, its total biomass yield Y_B and structural biomass yield Y_V differ, and they can be analytically represented as a function of specific growth rate μ only for an exponentially growing population.



3 Results of model comparisons

3.1 Predicted CUE-growth rate tradeoffs for exponentially growing populations

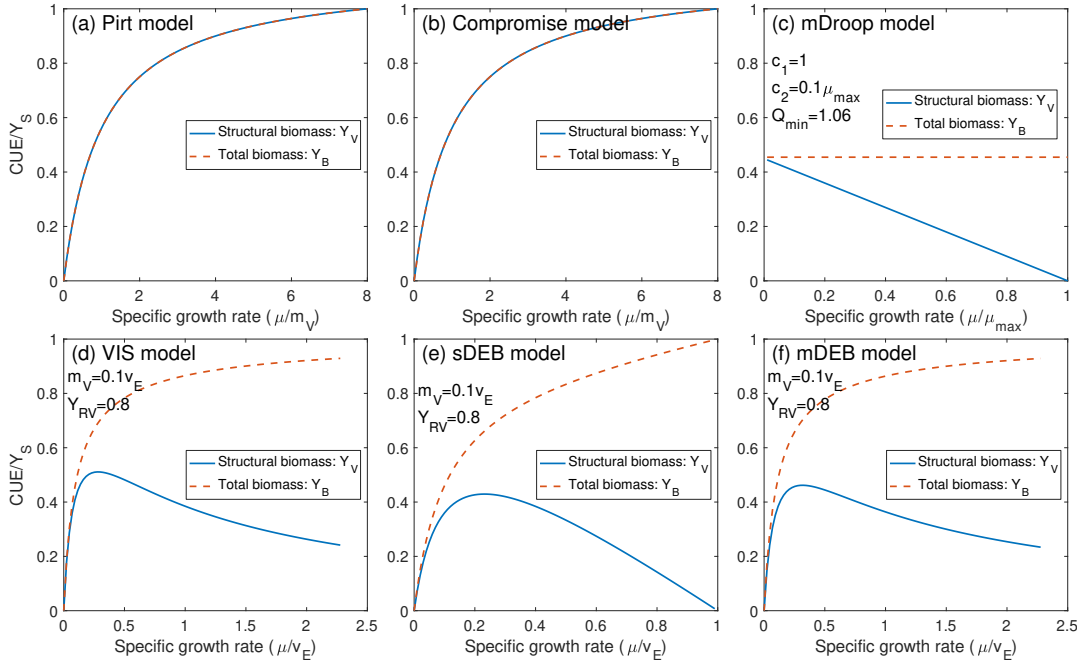


Figure 2. Comparison of relationships between CUE and specific growth rate predicted by the six models. Shown in panels (c)-(f) are parameter values to construct the plots. Structural biomass CUE Y_V is defined as the fraction of captured carbon substrate that is retained as structural biomass. Total biomass CUE Y_B is defined as the fraction of captured carbon substrate that is retained in structural and reserve biomass. Note that the specific growth rate for each model is normalized by parameters chosen by convenience.

For an exponentially growing population of biological cells, predictions by these six models can be sorted into three groups: (1) the Pirt and Compromise models predict that (both structural and total biomass) CUE increases asymptotically with increasing specific growth rate; (2) the mDroop model predicts that the total biomass CUE is insensitive to specific growth rate, while the structural biomass CUE decreases with increasing specific growth rate; and (3) the VIS, sDEB, and mDEB models predict that structural biomass CUE first increases then decreases with specific growth rate, while the total biomass CUE increases asymptotically with specific growth rate. Particularly, the increasing total biomass CUE as a function of specific growth rate aligns well with empirical measurements (e.g., Zheng et al., 2019; Hu et al., 2025; Collado et al., 2014), and the Pirt and Compromise models were specifically created to capture this feature observed in batch experiments (Pirt, 1965; Beftink et al., 1990). However, the Compromise model is argued to be more realistic than the Pirt model by allowing negative growth resulting from biomass degradation under low to no substrate conditions (Beftink et al., 1990; Wang and Post, 2012), while the Pirt model forces the growth rate to zero under the no-supply substrate condition.

3.2 Dynamic CUE in transient soil carbon dynamics under constant temperature

Among the six models, predicted relationships between total biomass CUE and specific growth rate can also be organized in three groups (Figure 3): (a) the Pirt and Compromise models predict essentially identical, almost linearly increasing, relationships (Figure 3a); (b) the mDroop model predicts a curve that traces like a pair of crossed-eyes (Figure 3b); and (c) the



VIS, sDEB, and mDEB models predict relationships look like baguettes that are slanting slightly up and to the right, and those by the two DEB models are nearly overlapping each other (Figure 3c). (The predicted soil carbon dynamics are presented in Figure S2, where their predictions again fall into three groups, even though the temporal variability of fast pool C, slow pool C, and total biomass are different but arguably quite consistent among all six models by our choice to share as many parameters as possible among the models. Note that the use of fast and slow pools here simply means the former carbon substrate is kinetically more favorable than the latter to the microbes, and they do not have the same meaning as in microbe-implicit models, which are directly associated with turnover times (Parton et al., 1988).)

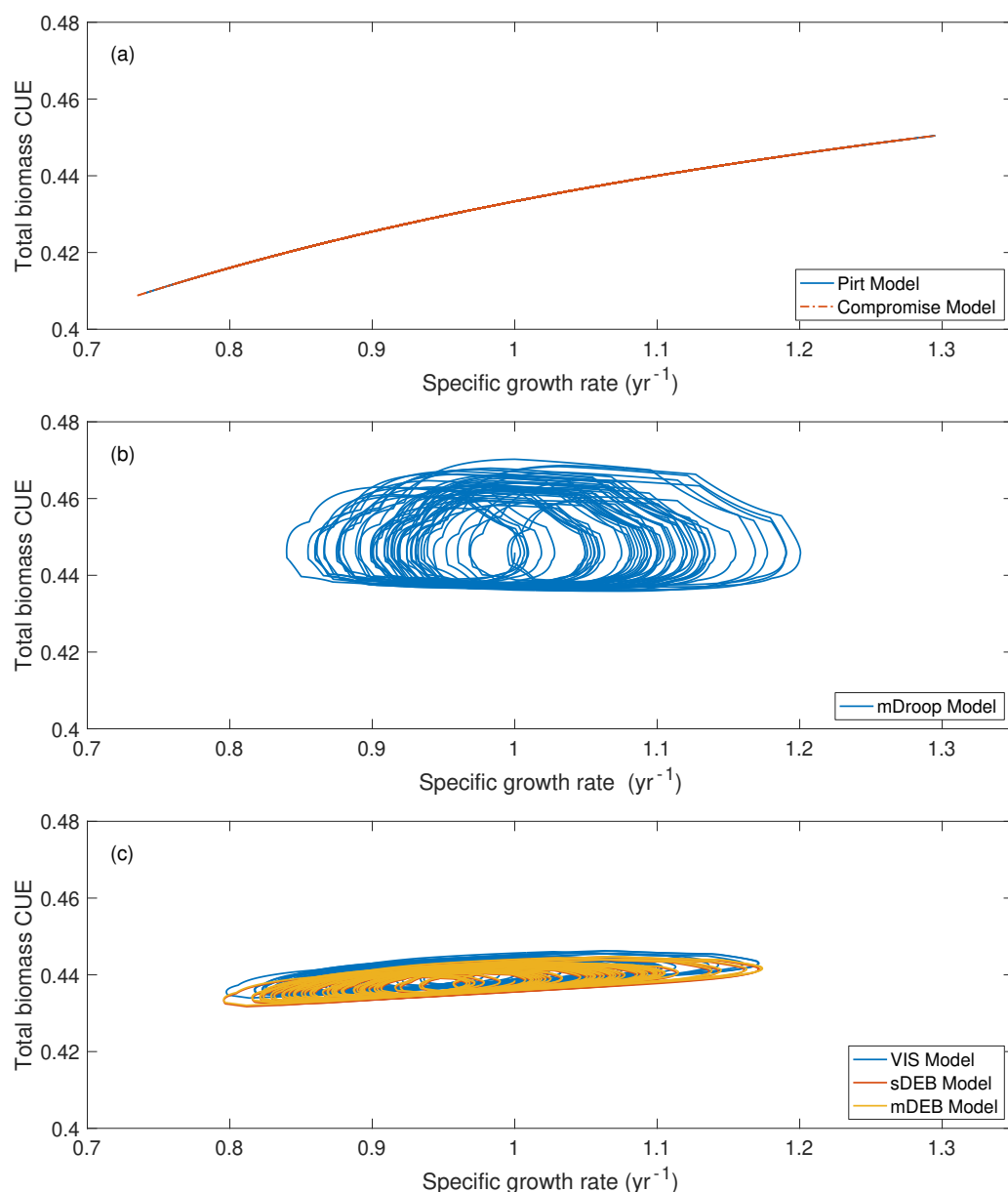


Figure 3. Relationship between total biomass CUE and specific growth rate. The evolution of different microbial carbon pools and total microbial biomass is presented in Figure S2 in the supplemental material. Note that results for the Pirt model and the Compromise model overlap each other in panel (a).



Since the Pirt and Compromise models each have only one biomass pool, their predicted microbes have only one CUE for each specific growth rate (Figure 3a). In contrast, the representation of reserve biomass makes the other four models predict multiple total biomass CUE values for each specific growth rate (Figure 3b, c) due to the non-repeating growth pattern (Figure S2d) driven by different year-to-year carbon input (Figure S2a).

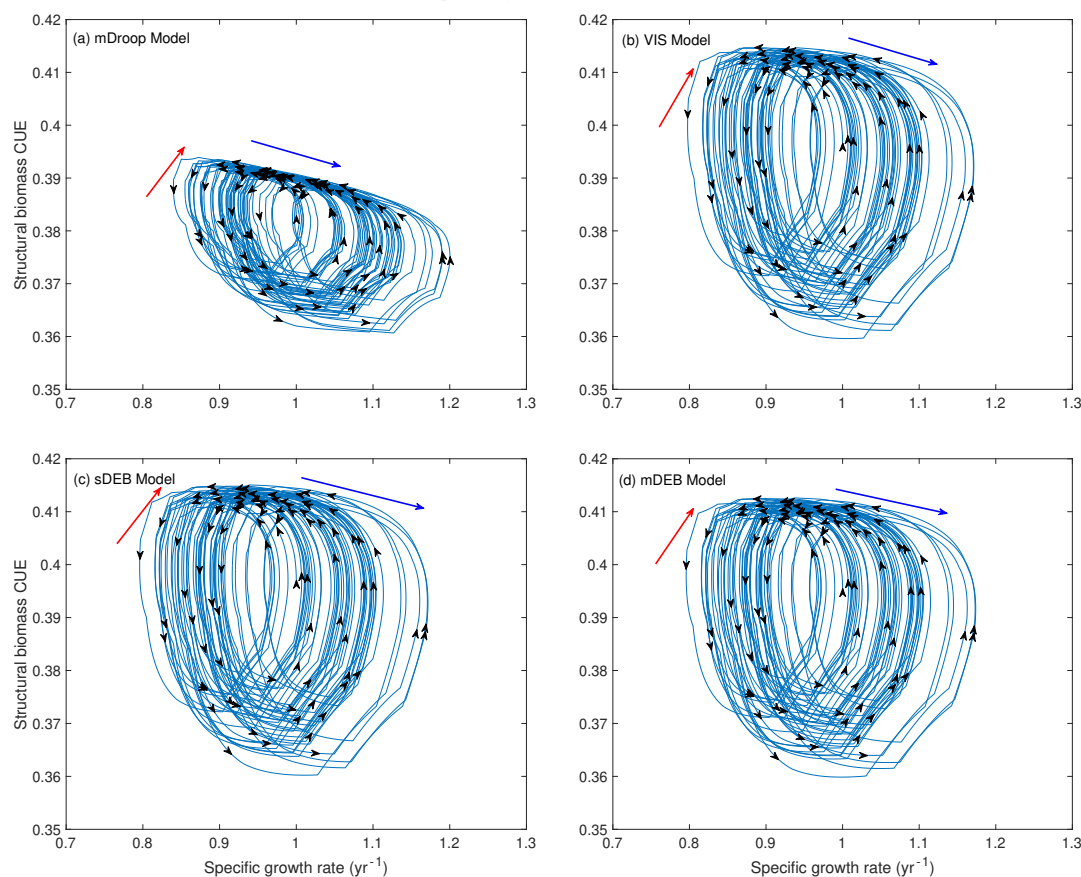


Figure 4. Relationship between structural biomass carbon use efficiency (CUE) and specific growth rate. In all panels, blue arrows indicate the period when structural biomass CUE decreases with specific growth rate, while red arrows indicate the period when structural biomass CUE increases with specific growth rate. Black arrows in the figure panels indicate the temporal progression in the simulations.

When the structural biomass CUE is analyzed with respect to the specific growth rate (Figure 4), the mDroop model predicts this relationship to have a right-downward slanting beehive shape (Figure 4a). Meanwhile, the VIS, sDEB, and mDEB models all predict the relationship to be more like an apple (Figure 4b, c, d). In all, just like that for the total biomass CUE, these four models predict that there is not a one-to-one relationship between structural biomass CUE and specific growth rate under constant temperature and month-to-month varying carbon input.

3.3 Dynamic CUE in transient state soil carbon dynamics under day-to-day varying temperatures

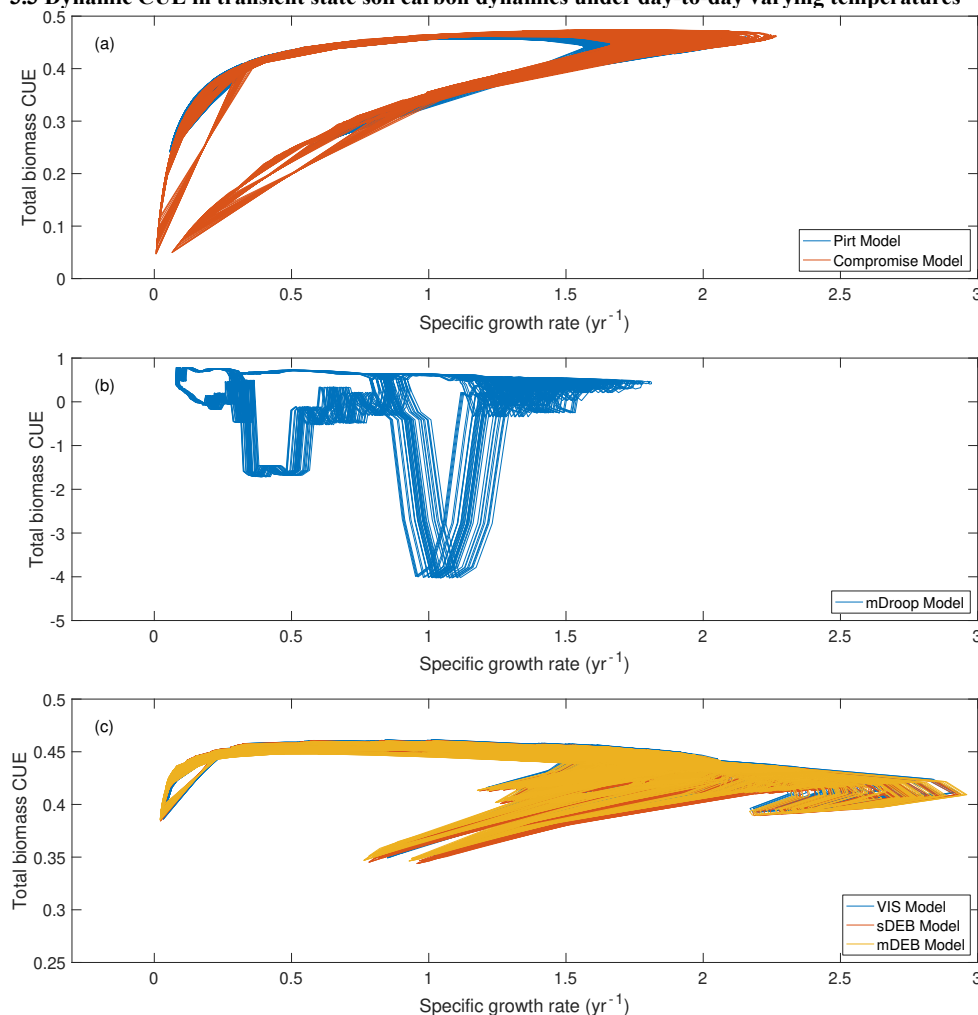


Figure 5. Variation of total biomass CUE with respect to specific growth rate. Data are extracted from the last 40 years of the 50-year simulations driven by month-to-month varying carbon input and day-to-day varying temperatures. The corresponding soil carbon dynamics are shown in Figure S3 in the supplemental material.

When the temperature effect on kinetic parameters is further considered (on top of the 50-year month-to-month variable carbon input), we find much richer variation of the relationship between total biomass CUE and specific growth rate. Still, the predicted relationships can be organized into the same three groups: (a) those by the Pirt and Compromise models (Figure 5a), which look like a toucan's head, (b) that by the mDroop model (Figure 5b), which looks like a left-looking dog that has unusually strong rear legs and a fluffy tail, and (c) those by the VIS, sDEB, and mDEB models (Figure 5c), which look like heads of right-looking eagles. Among these three groups, the relationship predicted by the mDroop model has the largest spread. In particular, the mDroop model predicts significant occurrence of negative CUE, where excessive maintenance cost leads to the loss of biomass in the presence of active carbon substrate uptake. Meanwhile, predictions by the VIS, sDEB, and mDEB models show a much tighter spread, and, due to the chosen parameter combinations, do not involve negative CUE (Figure 5c) as also found for the Pirt and Compromise models (Figure 5a). Nonetheless, by considering temporally varying carbon inputs and temperatures, one specific growth rate can correspond to many values of CUE.



When the relationship between total biomass CUE and temperature is analyzed, the patterns obtained are even more complex (Figure 6). (Note that temperature was varied daily, and repeated over the 50-year simulation period.) The Pirt and Compromise models both show a pattern of larger spread at low and high temperatures, and a general pattern that (looks like an iron bridge and) first increases and then decreases with temperature (Figure 6a). The relationships predicted by the VIS, sDEB, and mDEB models have a much tighter pattern and smaller variation (Figure 6c), a phenomenon that is consistent with observations that biological organisms evolutionarily develop reserve dynamics to stabilize performance (thereby less variable CUE) in the presence of fluctuating environmental conditions (Kooijman, 2009). Predictions by the mDroop model show the largest variation, with CUE-temperature curves aggregated into many distorted stripes, and the spread are largest under low temperature, followed by high and intermediate temperatures (Figure 6b). Overall, all models predict that there are many CUE values at any given temperature.

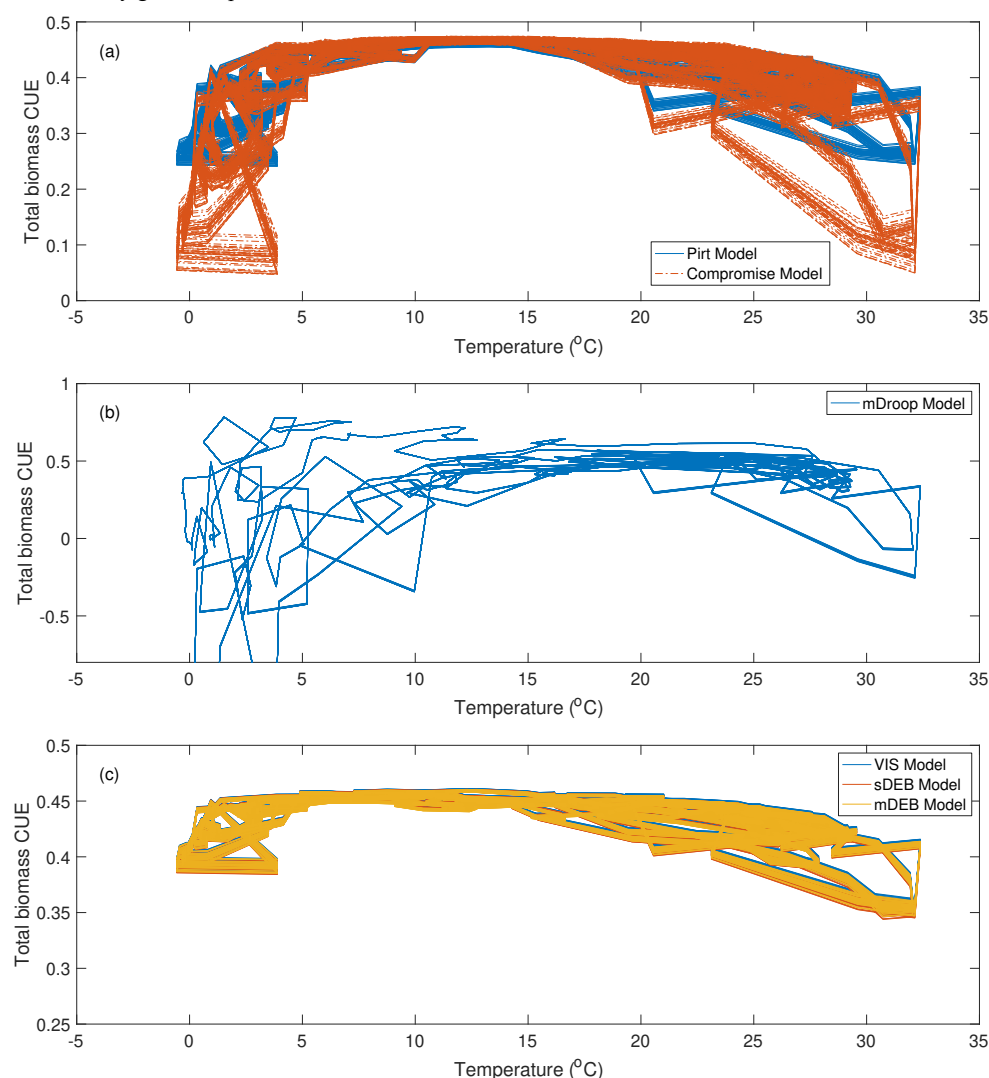


Figure 6. Variation of total biomass CUE with respect to temperature for different models. Results were plotted using the last 40 years of the 50-year simulations (shown in Figure S3).



265 4 Discussion

4.1 No deterministic relationship of CUE with respect to specific growth rate, or other environmental factors

It has long been recognized that CUE has a strong control on carbon and nutrient cycling through biological organisms and their host systems. However, many existing microbial models treat CUE as either a constant or a function depending deterministically on its controlling factors (Allison et al., 2010; Wang et al., 2021; He et al., 2015; Wieder et al., 2015). Our analysis here suggests that due to the indirect connection between maintenance respiration and substrate uptake, under time-varying conditions (like the varying carbon input and temperature considered here), there is not likely a deterministic relationship between CUE and its controlling factors or specific growth rate. Therefore, depending on the sampling time and location (e.g. the line segments indicated by blue or red arrows in the figures), as well as the averaging method involved in analysis (Tang and Riley, 2015), we may find CUE to have various trends with respect to the controlling variable being investigated (He et al., 2024). While it is not investigated here how much the simulated soil organic matter dynamics will change if the CUE is otherwise parameterized with a deterministic function, based on results from Tang and Riley (2015), we expect the change will be significant. In all, we contend that CUE should be resolved dynamically by explicitly representing the acquired carbon use for processes other than assimilation. This representation has been generally adopted in plant growth models, and soil biogeochemical models should also adopt it to ensure the mechanistic coherency of the overall ecosystem models.

4.2 The mDEB model seems to be superior for representing general biological growth

In the literature, due to their simple mathematical formulation and relatively good performance, the Pirt and Compromise models have been used much more frequently than the other four models in modeling microbes and plants. For instance, the land component (ELM) of the Energy Exascale Earth Model (Zhu et al., 2019) represents plant growth in a form that resembles the Compromise model, where new structural growth is driven by the residual gross primary productivity flux after subtracting the carbon requirement for maintenance and storage-replenishment. This source driven approach is also adopted by the Biome model (Weng et al., 2019) and the FATES model (Knox et al., 2024). We note that, in order to match observed nighttime root growth, the relative demand configuration in ELM has to introduce a carbon storage pool that may often become (unrealistically) negative at night and be replenished by new photosynthates in the following daytime (Burrows et al., 2020). Sierra et al. (2022) criticized that this source driven approach may lead to overly fast plant carbon turnover as indicated by a modeled too young radiocarbon signal in plant respiration compared to observations. Meanwhile, it has long been advocated that plant growth is better modeled using the sink driven approach, where carbon storage drives the growth of plant organs, and photosynthesis effects growth indirectly through replenishing the carbon storage (Fatichi et al., 2014; Fourcaud et al., 2008). Our analysis here suggests that the Pirt and Compromise models, although treating growth as driven directly by substrate uptake, are able to produce very rich variation in microbial CUE when analyzed with respect to either specific growth rates or temperatures (Figure 5a and Figure 6a). Interestingly but not surprisingly, their predicted CUE patterns vary more widely than those predicted by the VIS, sDEB, and mDEB models (Figure 5c and Figure 6c), where structural biomass growth is sink driven as fueled by reserve biomass, which is evolutionarily developed by biological organisms to stabilize their metabolic performance in the face of environmental fluctuations (Kooijman, 2009). Note that the VIS model considers maintenance respiration and growth as two-parallel processes of equal priority, while the sDEB and mDEB models regard maintenance to have priority over growth. Thus, at the cellular level, the VIS model seems to be mechanistically less reasonable by triggering earlier death through maintenance and growth competition.



Our analysis indicates that only the sink-driven models (i.e. the VIS model and two DEB models) are able to capture the feature that structural biomass CUE first increases and decreases with specific growth rate as inferred from the synthesis of empirical observations (Lipson, 2015). However, if one chooses the mDroop model, which represents biological growth as sink driven only apparently (because it computes the carbon quota based on total biomass, rather than reserve biomass, to drive the growth), then the predicted transient CUE dynamics can be quite different (Figure 5 and Figure 6), which are likely to be more easily falsified empirically. Nonetheless, when exponential growth is considered, the VIS, sDEB, and mDEB models are found to be more consistent with the Odum-Pinkerton model (Odum and Pinkerton, 1955) that is formulated using non-equilibrium thermodynamics. Our numerical analysis here shows that the VIS, sDEB and mDEB models are equally good (as evidenced by their very similar performance for all cases analyzed here), because maintenance respiration is usually a small fraction of total respiration. As the VIS model was initially proposed to model plant growth (Thornley, 1972), we hypothesize that the sDEB and mDEB models would be comparably good for modeling plant growth. Additionally, if we consider previous comparisons between the sDEB and mDEB models (Tang and Riley, 2025), then with its better mechanistic coherency and higher efficiency in numerical solution, the mDEB model seems to be a better formulation for representing biological growth under general conditions.

5 Conclusions

By starting from non-equilibrium thermodynamics, we infer that under no change of internal energy storage density (as usually is the case for internal combustion engines), the power use efficiency of a thermal engine as defined by the ratio of useful power output and power input will first increase, then plateau and finally decrease with increasing input power. Following this, we deduced that (which was also inferred by (Lipson, 2015) based on a synthesis of empirical observations), for an exponentially growing population of cells, the relationship between structural biomass carbon use efficiency and specific growth rate should follow the same pattern. In our analysis of six biological growth models adopted in currently popular ecosystem biogeochemical models, we found that only the VIS, sDEB, and mDEB models correctly capture this relationship. Considering transient carbon inputs and temperatures, all six models suggest that there is not a deterministic relationship of carbon use efficiency with respect to specific growth rate, substrate uptake rate, carbon inputs, or temperature. Therefore, combining with our previous analysis (Tang and Riley, 2015), we contend that, in order to robustly simulate the emergent carbon use efficiency dynamics and its consequent influence on ecosystem biogeochemistry, models should represent biological growth as sink-driven, and the effect of controlling factors like temperature and moisture should not be applied as multiplier functions, rather they should be applied to directly modify the kinetic parameters of different metabolic processes. Our analysis shows that the mDEB model is a good candidate framework to meet all these needs, and will potentially help ecosystem biogeochemistry models to improve their simulated variability of ecosystem dynamics in response to changing driving conditions.

Appendix A: Nomenclature

Table A1: Definition of symbols used in the modified Odum-Pinkerton model and models in Table 1.

Symbol	Unit	Description
c	Application dependent	Parameter for the modified Odum-Pinkerton model
c_1	None	Salting parameter for growth respiration in mDroop model
c_2	year ⁻¹	Scaling parameter for maintenance respiration in mDroop model
f	Application dependent	Parameter for the modified Odum-Pinkerton model



$h(S)$	None	Substrate response function in Pirt model and Compromise model
$j_A(S)$	year ⁻¹	Specific substrate uptake in the mDroop model, VIS model and DEB models.
l	Application dependent	Parameter for the modified Odum-Pinkerton model
m_V	year ⁻¹	Specific maintenance respiration rate for Pirt model, Compromise model, VIS model, and DEB models
p	None	Normalized input power in the modified Odum-Pinkerton model
$q(S)$	year ⁻¹	Specific substrate uptake rate in all growth models
v_E	year ⁻¹	Specific reserve mobilization rate in the VIS model and DEB models
J_1	Application dependent	Input flux in the modified Odum-Pinkerton model
J_2	Application dependent	Input flux in the modified Odum-Pinkerton model
P_1	Application dependent	Input power in the modified Odum-Pinkerton model
P_2	Application dependent	Useful output power in the modified Odum-Pinkerton model
Q_{min}	None	Minimum carbon quota for growth in the mDroop model
Q_{max}	None	Maximum carbon quota for growth in the mDroop model
S	gC m ⁻²	Substrate concentration in the growth models
S_e	J K ⁻¹	Entropy
T	K	Temperature
X_1, X_2	Application dependent	Forces in the modified Odum-Pinkerton model
Y_{RV}	None	Conversion efficiency from reserve biomass to structural biomass in VIS model and DEB models
Y_S	None	Substrate assimilation efficiency in all models
Y_V	None	Structural biomass carbon use efficiency in all models
Y_B	None	Total biomass carbon use efficiency in all models
ϵ	Application dependent	Parameter for the modified Odum-Pinkerton model
η	None	Power efficiency in the modified Odum-Pinkerton model
μ_{max}		Maximum specific growth rate in the Pirt model, Compromise model and mDroop model
$\mu(S)$		Specific growth rate in all growth models



Author contributions.

JYT formulated the idea, conduct the analysis and wrote the paper. WJR, GM, ELB discussed the results and edited the manuscript.

Competing interests.

340 The contact author has declared that neither of the authors has any competing interests

Code/data availability.

The code and data used in this study are available at: https://github.com/jinyuntang/cue_paper.

Disclaimer.

345 Financial support does not constitute an endorsement by the Department of Energy and National Science Foundation of the views expressed in this study.

Financial support.

The research was supported by the director of the Office of Science, Office of Biological and Environmental Research, of the US Department of Energy (contract no. DEAC02-05CH11231) and the National Science Foundation (grant no. 2125069).

350 Reference

- Allison, S. D.: Rethinking microbial carbon use efficiency in soil models, *Nature Climate Change*, 15, 10-12, 10.1038/s41558-024-02217-6, 2025.
- Allison, S. D., Wallenstein, M. D., and Bradford, M. A.: Soil-carbon response to warming dependent on microbial physiology, *Nat Geosci*, 3, 336-340, 10.1038/Ngeo846, 2010.
- 355 Andresen, B., Salamon, P., and Berry, R. S.: Thermodynamics in finite-time, *Phys Today*, 37, 62-70, 10.1063/1.2916405, 1984.
- Andresen, B., Berry, R. S., Nitzan, A., and Salamon, P.: Thermodynamics in finite time .1. Step-Carnot cycle, *Phys Rev A*, 15, 2086-2093, 10.1103/PhysRevA.15.2086, 1977.
- Beefink, H. H., Vanderheijden, R. T. J. M., and Heijnen, J. J.: Maintenance requirements - energy supply from simultaneous endogenous respiration and substrate consumption, *Fems Microbiol Ecol*, 73, 203-209, 10.1016/0378-1097(90)90731-5, 1990.
- 360 Bejan, A.: Entropy generation minimization: The new thermodynamics of finite-size devices and finite-time processes, *J Appl Phys*, 79, 1191-1218, 10.1063/1.362674, 1996.
- Bloom, A. A., Exbrayat, J. F., van der Velde, I. R., Feng, L., and Williams, M.: The decadal state of the terrestrial carbon cycle: Global retrievals of terrestrial carbon allocation, pools, and residence times, *P Natl Acad Sci USA*, 113, 1285-1290, 10.1073/pnas.1515160113, 2016.
- 365 Boland, B. and Schreyer, S.: The Relationship Between Horsepower & Fuel Efficiency, 2024.
- Burrows, S. M., Maltrud, M., Yang, X., Zhu, Q., Jeffery, N., Shi, X., Ricciuto, D., Wang, S., Bisht, G., Tang, J., Wolfe, J., Harrop, B. E., Singh, B., Brent, L., Baldwin, S., Zhou, T., Cameron-Smith, P., Keen, N., Collier, N., Xu, M., Hunke, E. C., Elliott, S. M., Turner, A. K., Li, H., Wang, H., Golaz, J. C., Bond-Lamberty, B., Hoffman, F. M., Riley, W. J., Thornton, P. E., Calvin, K., and Leung, L. R.: The DOE E3SM v1.1 Biogeochemistry configuration: description and simulated ecosystem-climate responses to historical changes in forcing, *J Adv Model Earth Sy*, 12, ARTN e2019MS001766 10.1029/2019MS001766, 2020.
- 370 Collado, S., Rosas, I., González, E., Gutierrez-Lavin, A., and Diaz, M.: response in membrane bioreactors under salicylic acid-induced stress conditions, *J Hazard Mater*, 267, 9-16, 10.1016/j.jhazmat.2013.12.034, 2014.
- Dawes, E. A. and Ribbons, D. W.: Some aspects of endogenous metabolism of bacteria, *Bacteriol Rev*, 28, 126-149, 10.1128/Mmbr.28.2.126-149.1964, 1964.
- 375 Fatichi, S., Leuzinger, S., and Körner, C.: Moving beyond photosynthesis: from carbon source to sink-driven vegetation modeling, *New Phytol*, 201, 1086-1095, 10.1111/nph.12614, 2014.
- Feynman, R. P., Leighton, R. B., and Sands, M.: The Feynman Lectures on Physics, The New Millennium Edition, Basic Books2011.
- Fourcaud, T., Zhang, X., Stokes, A., Lambers, H., and Körner, C.: Plant growth modelling and applications:: The increasing importance of plant architecture in growth models, *Ann Bot-London*, 101, 1053-1063, 10.1093/aob/mcn050, 2008.
- 380 He, X. J., Abs, E., Allison, S. D., Tao, F., Huang, Y. Y., Manzoni, S., Abramoff, R., Bruni, E., Bowring, S. P. K., Chakrawal, A., Ciais, P., Elsgaard, L., Friedlingstein, P., Georgiou, K., Hugelius, G., Holm, L. B., Li, W., Luo, Y. Q., Marmasse, G., Nunan, N.,



- Qiu, C. J., Sitch, S., Wang, Y. P., and Goll, D. S.: Emerging multiscale insights on microbial carbon use efficiency in the land carbon cycle, *Nat Commun*, 15, ARTN 8010 10.1038/s41467-024-52160-5, 2024.
- 385 He, Y. J., Yang, J. Y., Zhuang, Q. L., Harden, J. W., McGuire, A. D., Liu, Y. L., Wang, G. S., and Gu, L. H.: Incorporating microbial dormancy dynamics into soil decomposition models to improve quantification of soil carbon dynamics of northern temperate forests, *J Geophys Res-Bioge*, 120, 2596-2611, 10.1002/2015jg003130, 2015.
- Hu, J. X., Cui, Y. X., Manzoni, S., Zhou, S. X., Cornelissen, J. H. C., Huang, C. D., Schimel, J., and Kuzyakov, Y.: Microbial carbon use efficiency and growth rates in soil: global patterns and drivers, *Global Change Biol*, 31, ARTN e70036 10.1111/gcb.70036, 2025.
- 390 Jenkinson, D. S.: The turnover of organic-carbon and nitrogen in soil, *Philos T R Soc B*, 329, 361-368, 10.1098/rstb.1990.0177, 1990.
- Knox, R. G., Koven, C. D., Riley, W. J., Walker, A. P., Wright, S. J., Holm, J. A., Wei, X. Y., Fisher, R. A., Zhu, Q., Tang, J. Y., Ricciuto, D. M., Shuman, J. K., Yang, X. J., Kueppers, L. M., and Chambers, J. Q.: Nutrient dynamics in a coupled terrestrial biosphere and land model (ELM-FATES-CNP), *J Adv Model Earth Sy*, 16, ARTN e2023MS003689 10.1029/2023MS003689, 2024.
- 395 Kooijman, S. A. L. M.: *Dynamic Energy Budget Theory for Metabolic Organisation*, Cambridge University Press, Cambridge, 10.1017/CBO9780511805400, 2009.
- Koven, C. D., Riley, W. J., Subin, Z. M., Tang, J. Y., Torn, M. S., Collins, W. D., Bonan, G. B., Lawrence, D. M., and Swenson, S. C.: The effect of vertically resolved soil biogeochemistry and alternate soil C and N models on C dynamics of CLM4, *Biogeosciences*, 10, 7109-7131, 10.5194/bg-10-7109-2013, 2013.
- 400 Lipson, D. A.: The complex relationship between microbial growth rate and yield and its implications for ecosystem processes, *Front Microbiol*, 6, ARTN 615 10.3389/fmicb.2015.00615, 2015.
- Liu, Z. G., Chen, Z., Yu, G. R., Yang, M., Zhang, W. K., Zhang, T. Y., and Han, L.: Ecosystem carbon use efficiency in ecologically vulnerable areas in China: Variation and influencing factors, *Front Plant Sci*, 13, ARTN 1062055 10.3389/fpls.2022.1062055, 2022.
- 405 Manzoni, S., Capek, P., Porada, P., Thurner, M., Winterdahl, M., Beer, C., Brüchert, V., Frouz, J., Herrmann, A. M., Lindahl, B. D., Lyon, S. W., Santrucková, H., Vico, G., and Way, D.: Reviews and syntheses: Carbon use efficiency from organisms to ecosystems - definitions, theories, and empirical evidence, *Biogeosciences*, 15, 5929-5949, 10.5194/bg-15-5929-2018, 2018.
- 410 Monteiro, M., Stari, C., Cabeza, C., and Marti, A. C.: The Atwood machine revisited using smartphones, *Phys Teach*, 53, 373-374, 10.1119/1.4928357, 2015.
- Nev, O. A. and van den Berg, H. A.: Variable-Internal-Stores models of microbial growth and metabolism with dynamic allocation of cellular resources, *J Math Biol*, 74, 409-445, 10.1007/s00285-016-1030-4, 2017.
- 415 Odum, H. T. and Pinkerton, R. C.: Times speed regulator - the optimum efficiency for maximum power output in physical and biological systems, *Am Sci*, 43, 331-343, 1955.
- Onsager, L.: Reciprocal relations in irreversible processes. II., *Phys Rev*, 38, 2265-2279, 10.1103/PhysRev.38.2265, 1931a.
- Onsager, L.: Reciprocal relations in irreversible processes. I., *Phys Rev*, 37, 405-426, 10.1103/PhysRev.37.405, 1931b.
- Parton, W. J., Stewart, J. W. B., and Cole, C. V.: Dynamics of C, N, P and S in grassland soils - a model, *Biogeochemistry*, 5, 109-131, 10.1007/Bf02180320, 1988.
- 420 Pirt, S. J.: Maintenance energy of bacteria in growing cultures, *Proc R Soc Ser B-Bio*, 163, 224-231, 10.1098/rspb.1965.0069, 1965.
- Pirt, S. J.: Maintenance energy - a general-model for energy-limited and energy-sufficient growth, *Arch Microbiol*, 133, 300-302, 10.1007/Bf00521294, 1982.
- 425 Roach, T. N. F., Salamon, P., Nulton, J., Andresen, B., Felts, B., Haas, A., Calhoun, S., Robinett, N., and Rohwer, F.: Application of finite-time and control thermodynamics to biological processes at multiple scales, *J Non-Equil Thermody*, 43, 193-210, 10.1515/jnet-2018-0008, 2018.
- Sierra, C. A., Ceballos-Núñez, V., Hartmann, H., Herrera-Ramírez, D., and Metzler, H.: Ideas and perspectives: Allocation of carbon from net primary production in models is inconsistent with observations of the age of respired carbon, *Biogeosciences*, 19, 3727-3738, 10.5194/bg-19-3727-2022, 2022.
- 430 Sinsabaugh, R. L., Moorhead, D. L., Xu, X. F., and Litvak, M. E.: Plant, microbial and ecosystem carbon use efficiencies interact to stabilize microbial growth as a fraction of gross primary production, *New Phytol*, 214, 1518-1526, 10.1111/nph.14485, 2017.
- Tang, J. Y. and Riley, W. J.: Weaker soil carbon-climate feedbacks resulting from microbial and abiotic interactions, *Nature Climate Change*, 5, 56-60, 10.1038/Nclimate2438, 2015.
- Tang, J. Y. and Riley, W. J.: Revising the dynamic energy budget theory with a new reserve mobilization rule and three example applications to bacterial growth, *Soil Biol Biochem*, 178, ARTN 108954 10.1016/j.soilbio.2023.108954, 2023.
- 435 Tang, J. Y. and Riley, W. J.: Technical note: A modified formulation of dynamic energy budget theory for faster computation of biological growth, *Biogeosciences*, 22, 1809-1819, 10.5194/bg-22-1809-2025, 2025.
- Tao, F., Huang, Y. Y., Hungate, B. A., Manzoni, S., Frey, S. D., Schmidt, M. W. I., Reichstein, M., Carvalhais, N., Ciais, P., Jiang, L. F., Lehmann, J., Wang, Y. P., Houlton, B. Z., Ahrens, B., Mishra, U., Hugelius, G., Hocking, T. D., Lu, X. J., Shi, Z., Viatkin, K., Vargas, R., Yigini, Y., Omuto, C., Malik, A. A., Peralta, G., Cuevas-Corona, R., Di Paolo, L. E., Luotto, I., Liao, C. J., Liang, Y. S., Saynes, V. S., Huang, X. M., and Luo, Y. Q.: Microbial carbon use efficiency promotes global soil carbon storage, *Nature*, 618, 981-985, 10.1038/s41586-023-06042-3, 2023.
- 440



- Thingstad, T. F.: Utilization of N, P, and organic C by heterotrophic bacteria .1. Outline of a chemostat theory with a consistent concept of maintenance metabolism, *Mar Ecol Prog Ser*, 35, 99-109, 10.3354/meps035099, 1987.
- 445 Thornley, J. H. M.: A balanced quantitative model for root: shoot ratios in vegetative plants, *Ann. Bot.*, 36, 431-441, 10.1093/oxfordjournals.aob.a084602, 1972.
- Wang, G. S. and Post, W. M.: A theoretical reassessment of microbial maintenance and implications for microbial ecology modeling, *Fems Microbiol Ecol*, 81, 610-617, 10.1111/j.1574-6941.2012.01389.x, 2012.
- Wang, Y. P., Zhang, H. C., Ciais, P., Goll, D., Huang, Y. Y., Wood, J. D., Ollinger, S. V., Tang, X. L., and Prescher, A. K.:
 450 Microbial activity and root carbon inputs are more important than soil carbon diffusion in simulating soil carbon profiles, *J Geophys Res-Bioge*, 126, ARTN e2020JG006205 10.1029/2020JG006205, 2021.
- Weng, E. S., Dybzinski, R., Farrior, C. E., and Pacala, S. W.: Competition alters predicted forest carbon cycle responses to nitrogen availability and elevated CO₂: simulations using an explicitly competitive, game-theoretic vegetation demographic model, *Biogeosciences*, 16, 4577-4599, 10.5194/bg-16-4577-2019, 2019.
- 455 Wieder, W. R., Grandy, A. S., Kallenbach, C. M., Taylor, P. G., and Bonan, G. B.: Representing life in the Earth system with soil microbial functional traits in the MIMICS model, *Geosci Model Dev*, 8, 1789-1808, 10.5194/gmd-8-1789-2015, 2015.
- Williams, F. M.: A model of cell growth dynamics, *J Theor Biol*, 15, 190-207, Doi 10.1016/0022-5193(67)90200-7, 1967.
- Yuan, H., Ma, Y. H., and Sun, C. P.: Optimizing thermodynamic cycles with two finite-sized reservoirs, *Phys Rev E*, 105, ARTN L022101 10.1103/PhysRevE.105.L022101, 2022.
- 460 Zhang, Y. J., Xu, M., Chen, H., and Adams, J.: Global pattern of NPP to GPP ratio derived from MODIS data: effects of ecosystem type, geographical location and climate, *Global Ecol Biogeogr*, 18, 280-290, 10.1111/j.1466-8238.2008.00442.x, 2009.
- Zheng, Q., Hu, Y. T., Zhang, S. S., Noll, L., Böckle, T., Richter, A., and Wanek, W.: Growth explains microbial carbon use efficiency across soils differing in land use and geology, *Soil Biol Biochem*, 128, 45-55, 10.1016/j.soilbio.2018.10.006, 2019.
- 465 Zhu, Q., Riley, W. J., Tang, J. Y., Collier, N., Hoffman, F. M., Yang, X. J., and Bisht, G.: Representing nitrogen, phosphorus, and carbon interactions in the E3SM land model: development and global benchmarking, *J Adv Model Earth Sy*, 11, 2238-2258, 10.1029/2018ms001571, 2019.